BMB Reports - Manuscript Submission

Manuscript Draft

DOI: 10.5483/BMBRep.2022-0165

Manuscript Number: BMB-22-165

Title: Inhibition of the Semaphorin 4D-Plexin-B1 axis prevents calcification in vascular smooth muscle cells

Article Type: Article

Keywords: Semaphorin 4D; Plexin-B1; Vascular smooth muscle cells; Vascular calcification

Corresponding Author: Moon-Kyoung Bae

Authors: Hyun-Joo Park[1], Yeon Kim[1], Mi-Kyoung Kim[1], Hyung Joon Kim[1], Soo-Kyung Bae[1], Moon-Kyoung Bae[1,*]

Institution: [1]School of Dentistry, Pusan National University,

Manuscript Type: Article

Title: Inhibition of the Semaphorin 4D-Plexin-B1 axis prevents calcification in vascular smooth muscle cells

Author's name: Hyun-Joo Park[1,2,3], Yeon Kim[1,2,3], Mi-Kyoung Kim[1,2], Hyung Joon Kim[1,2,3], Soo-Kyung Bae[2,3,4], and Moon-Kyoung Bae[1,2,3*]

Affiliation: [1]Department of Oral Physiology, [2]Periodontal Disease Signaling Network Research Center (MRC), [3]Dental and Life Science Institute, [4]Department of Dental Pharmacology, School of Dentistry, Pusan National University, Yangsan 50612, South Korea

Running Title: Role of Semaphorin 4D in vascular calcification

***Corresponding author:** Moon-Kyoung Bae, Department of Oral Physiology, School of Dentistry, Pusan National University, Yangsan 50612, South Korea; Tel.: 82-51-510-8239; E-mail: mkbae@pusan.ac.kr

ABSTRACT

Vascular calcification is common in cardiovascular diseases including atherosclerosis, and is associated with an increased risk of pathological events and mortality. Some semaphorin family members play an important role in atherosclerosis. In the present study, we show that Semaphoring 4D/Sema4D and its Plexin-B1 receptor were significantly upregulated in calcified aorta of a rat chronic kidney disease model. Significantly higher Sema4D and Plexin-B1 expression was also observed during inorganic phosphate-induced calcification of vascular smooth muscle cells. Knockdown of Sema4D or Plexin-B1 genes attenuated both the phosphate-induced osteogenic phenotype of vascular smooth muscle cells, through regulation of SMAD1/5 signaling, as well as apoptosis of vascular smooth muscle cells, through modulation of the Gas6/Axl/Akt survival pathway. Taken together, our results offer new insights on the role of Sema4D and Plexin-B1 as potential therapeutic targets against vascular calcification.

Keywords: Semaphorin 4D; Plexin-B1; Vascular smooth muscle cells; Vascular calcification

INTRODUCTION

Vascular calcification, defined as the pathological deposition of calcium phosphate in the vasculature, is typically observed in elderly individuals, as well as in patients with atherosclerosis, chronic renal failure, and diabetes mellitus (1). Importantly, it is associated with an increased risk of cardiovascular disease and mortality (1). Vascular smooth muscle cells (VSMCs) play a pivotal role in the intervening calcification of blood vessels owing to their transdifferentiation into osteoblast-like cells or chondrocyte-like cells (2). This process is altered by disturbed mineral homeostasis, inflammation, oxidative stress, and an imbalance between promoters and inhibitors (3). Most dangerously, the calcification of VSMCs augments the risk of plaque instability and rupture in atherosclerosis (4).

Semaphorins belong to a large family of membrane-bound and secreted proteins originally identified in the nervous system as mediators of axonal guidance (5). Semaphorin 4D (Sema4D) was initially identified in immune cells as the CD100 antigen and binds to two types of receptors, the high-affinity Plexin-B1 receptor and low-affinity CD72 C-type lectin receptor (6). Sema4D-Plexin-B1 is a multifunctional ligand-cell surface receptor structure found in several tissues, including neurons, lymphocytes, vascular endothelial cells, and tumor cells, with a role played in different physiological and pathological situations (7). Sema4D is the first documented member of the semaphorin family to be involved in the development of atherosclerosis (8). This phenomenon has been proved based on the previous observations that Sema4D and its receptor signaling promotes monocyte adhesion to the vascular endothelium,

intraplaque angiogenesis, platelet activation, and thrombus formation (9-12).

In the present study, we investigated the role of Sema4D in phosphate-induced VSMC calcification and the calcified aorta of a chronic kidney disease (CKD) animal model, and its underlying mechanism in VSMCs.

RESULTS

Sema4D and Plexin-B1 expression increases during aortic calcification in a CKD model

To elucidate the role of Sema4D in vascular calcification *in vivo*, we used an adenine diet-induced CKD vascular calcification rat model (13). Blood biochemical parameters of CKD rats are summarized in Supplementary Table 1. Histological assessment by hematoxylin and eosin staining revealed a clear and neat arrangement of VSMCs in sham animals, but a disordered smooth muscle arrangement in the aortic tissue of CKD rats (Fig. 1A). Von Kossa and alizarin red S (ARS) staining disclosed an extensive medial calcification in the aortas derived from CKD rats compared to those from sham animals (Fig. 1A). This was confirmed by a significantly greater calcified area relative to the that observed in the aortas of CKD rats (Fig. 1B). Next, we investigated the levels of Sema4D and Plexin-B1 in calcified aortic tissues from CKD rats. Immunohistochemistry showed significantly higher Sema4D and Plexin-B1 expression in aortic tissues of CKD rats than in those of sham animals (Fig. 1C), which was confirmed by western blotting (Fig. 1D). At the same time, serum analysis using an enzyme-linked immunosorbent assay (ELISA) showed that the secreted Sema4D protein were also elevated in the CKD rats compared with the sham rats (Fig. 1E). Finally, quantitative real-time polymerase chain reaction (PCR) demonstrated a prominent increase in the Sema4D and Plexin-B1 mRNA expression in the thoracic aortas from CKD rats (Fig. 1F).

Elevated expression of Sema4D and Plexin-B1 in phosphate-induced VSMC calcification in vitro.

Inorganic phosphate (Pi) stimulates the calcification of VSMCs *in vitro* (14). Thus, we analyzed whether elevated Pi promoted VSMC calcification under our established experimental conditions. As expected, addition of 2.6 and 3.5 mM Pi caused calcium deposition (Fig. 2A); whereas 1.4 mM Pi, equivalent to the human physiological serum phosphate level, failed to induce calcification. Calcium content and alkaline phosphatase (ALP) activity, a molecular marker of vascular calcification, in VSMCs were also markedly elevated under calcifying conditions compared to normal conditions (Fig. 2B and 2C). Next, we estimated the levels of soluble Sema4D protein in VSMC calcification stimulated by Pi. Estimation of soluble Sema4D revealed a gradual increase in the amount of secreted Sema4D with the severity of Pi-induced VSMC calcification (Fig. 2D). Western blotting and quantitative real-time PCR confirmed the elevated protein (Fig. 2E) and mRNA (Fig. 2F) expression of Sema4D and Plexin-B1 in Pi-induced VSMC calcification.

Sema4D and Plexin-B1 silencing attenuates osteogenic differentiation during Pi-induced vascular calcification.

To assess whether inhibition of Sema4D and Plexin-B1 alleviated Pi-induced VMSC calcification, we silenced the Sema4D and Plexin-B1 expressions with small interfering RNA (siRNA). The siRNA knockdown efficiency was confirmed by a decrease in Sema4D and Plexin-B1 protein and mRNA levels (Supplementary Fig. 1). Importantly, their silencing reduced the calcium deposition significantly even under calcifying conditions (Fig. 3A), as well as calcium content in VSMCs (Fig. 3B). Similarly, the increased activity of ALP was markedly inhibited by the Sema4D and Plexin-B1 knockdown (Fig. 3C). Next, we evaluated the effect of targeted silencing on

the expression of contractile and osteogenic markers. As shown in Figure 3D, 3E and Supplementary Fig. 2, the increased protein expression of Runx2, a master transcription factor of osteoblast differentiation, was suppressed by Sema4D and Plexin-B1 siRNA; whereas the decreased level of calponin, a marker of the contractile phenotype, was completely reversed. In addition, Sema4D and Plexin-B1 silencing upregulated the calponin mRNA and downregulated the Runx2 mRNA expressions in VSMCs subjected to Pi-induced osteogenic differentiation (Fig. 3F). Previous reports along with ours have reported that the phosphorylation of SMAD1/5 activates osteogenic gene markers such as Runx2 during osteogenic differentiation of VMSCs (15,16). Accordingly, we investigated whether the knockdown of Sema4D and Plexin-B1 altered the phosphorylation of SMAD1/5 in calcified VSMCs. Indeed, silencing of these two proteins blocked the increased expression of phospho-SMAD1/5 (Fig. 3D).

Sema4D and Plexin-B1 knockdown suppresses VSMC apoptosis and matrix vesicle release during vascular calcification.

Given that apoptosis plays a pivotal role in the initiation of vascular calcification (17), we assessed the extent of apoptosis in VSMCs using propidium iodide staining and the TUNEL assay. Compared with non-transfected cells, Sema4D and Plexin-B1 knockdown significantly inhibited Pi-induced apoptosis in VSMCs, with the proportion of apoptotic cells decreasing by 16.3% or 13.5%, respectively (Fig. 4A). Likewise, the proportion of TUNEL-positive apoptotic cells was significantly reduced when calcified VSMCs were treated with Sema4D and Plexin-B1 siRNA (Fig. 4B and Supplementary Fig. 3). Next, we checked the effect of Sema4D and Plexin-B1 knockdown on the expression of pro-apoptotic and anti-apoptotic markers in calcified VSMCs. Sema4D and Plexin-B1

knockdown blocked the increase in cleaved caspase-3 induced by 2.6 mM Pi (Fig. 4C), while significantly stimulating Bcl2 in calcified VSMCs (Fig. 4C). Pi is known to downregulate the Gas6/Axl/PI3K/Akt survival pathway, leading to VSMC apoptosis and calcification (18). We found that the exposure to 2.6 mM Pi markedly downregulated the expression of Gas6 and Axl; however, this effect was abolished by Sema4D and Plexin-B1 silencing (Fig. 4C). Because the Gas6/Axl survival pathway is PI3K/Akt-dependent (19), we examined the effect of Sema4D and Plexin-B1 knockdown on the PI3K/Akt pathway in calcified VSMCs. As expected, silencing of Sema4D and Plexin-B1 blocked the Pi-induced dephosphorylation of PI3K and Akt (Fig. 4C). VSMC apoptosis favors the calcification of VSMCs by promoting the release of calcifying membrane-bound matrix vesicles (20). Therefore, to confirm the inhibitory action of Sema4D and Plexin-B1 silencing on the release of these vesicles, the matrix vesicles were isolated from calcified VSMC lysates by collagenase digestion. The release of matrix vesicles was enhanced in the presence of 2.6 mM Pi, but was significantly reversed by Sema4D and Plexin-B1 silencing (Fig. 4D). Finally, Sema4D and Plexin-B1 knockdown successfully counteracted the increased ALP activity observed within matrix vesicles released from calcified VSMCs (Fig. 4E).

DISCUSSION

Vascular calcification is often accompanied by loss of bone mineral density in patients with CKD (21). This apparent calcification paradox was first documented by the frequent association between atherosclerotic vascular calcification and osteoporosis in postmenopausal women (22). However, the underlying mechanism and common regulators of the bone-vascular axis have not yet been established. Sema4D, expressed in osteoclasts during osteoclastogenesis, inhibits the bone formation by interacting with Plexin-B1, which is expressed by osteoblasts (23). Not surprisingly, serum Sema4D levels correlate with the changes in osteoporosis in postmenopausal women (24). In this study, Sema4D was shown to be crucial for the regulation of phosphate-induced calcification in VSMCs and calcium deposition in the aortas. Inflammation leads to a common microenvironment for vascular mineralization and bone demineralization (25). Inflammatory cytokines trigger vascular calcification through ossification of VSMCs and endothelial-mesenchymal transition, as well as bone loss through increased bone resorption and decreased bone formation (26). In addition, we confirmed the increased levels of pro-inflammatory genes, including the interleukins IL-6 and IL-8, monocyte chemoattractant protein-1, and tumor necrosis factor-α, in calcified Pi-induced VSMCs. Soluble Sema4D levels in serum and body fluids have shown a positive correlation with the disease severity in chronic inflammatory disorders such as rheumatoid arthritis (27). The findings shown in the present study, together with previous observations, suggest that Sema4D may act as a common regulator linking bone disorders and vascular calcification.

Emerging evidence suggests that Sema4D-Plexin-B1 signaling is involved in the endothelial dysfunction of the vasculature. Sema4D regulates pathological retinal

neovascularization and endothelial permeability via Plexin-B1 (28). Sema4D expressed in endothelial cells mediated monocytes adhesion to the endothelial cells, a critical step in vascular inflammation, by interaction with Plexin-B1 (10). Additionally, Sema4D controls migration, as well as pro-angiogenic and pro-inflammatory responses in the endothelium (9,29). In comparison, little attention has been paid to the potential role of Sema4D-Plexin-B1 in the vascular dysfunction of VSMCs, the predominant vascular cell type. The present results provide first-time evidence that Sema4D-Plexin-B1 signaling is crucial for the regulation of mineralization and apoptosis in VSMCs during vascular calcification. Growing evidence suggests that communication between vascular endothelial cells and VSMCs is important for osteogenic differentiation of VSMCs during vascular calcification. Receptor activator of nuclear factor kappa beta-ligand stimulates osteoblastic activity of VSMCs by inducing the release of BMP-2 from endothelial cells in a paracrine manner (30). Conditioned medium from endothelial cells or co-culture with endothelial cells reinforces the calcification of VSMCs through the upregulation of IL-8 or matrix metalloproteinases (31,32). Future studies will determine whether Sema4D expressed in endothelial cells mediates the osteogenic differentiation of VSMCs when coupled to Plexin-B1.

Hyperphosphatemia, a key risk factor associated with atherosclerotic calcification in CKD, leads to excessive reactive oxygen species (ROS) production in patients and CKD animal models (33). Increased ROS generation triggers the cellular activation of osteo/chondrogenic signaling pathways, which are implicated in osteogenic conversion of VSMCs (34). Proper modulation of the redox status through inhibition or elimination of ROS production represents a potential therapeutic strategy in the prevention of VSMC calcification and the associated risk of cardiovascular disease (35). In this study, we

observed that silencing of Sema4D or Plexin-B1 decreased the Pi-induced ROS generation in VSMCs (data not shown). Therefore, it is possible that blocking of the Sema4D-Plexin-B1 axis could protect against ROS-mediated vascular calcification and these possibilities are under investigation.

In conclusion, the present study identified a novel function for the Sema4D-Plexin-B1 axis in vascular calcification. Moreover, we demonstrate that the inhibition of Sema4D and Plexin-B1 attenuates the osteoblastic differentiation in VSMCs through SMAD1/5 signaling, as well as VSMC apoptosis through Gas6/Axl/Akt signaling. These findings provide new evidence supporting the use of Sema4D-Plexin-B1 as a therapeutic target of vascular calcification in atherosclerosis or CKD.

MATERIALS AND METHODS

Further detailed information is provided in the Supplementary Information.

ACKNOWLEDGMENTS

This research was supported by grants from the National Research Foundation of Korea funded by the Korean government (MSIT, NRF-2018R1A5A2023879 and 2021R1A2C1003687).

CONFLICTS OF INTEREST

The authors declare no conflicts of interest.

FIGURE LEGENDS

Figure 1. Sema4D and Plexin-B1 expression in calcified aorta of CKD rats. (A) Representative photomicrographs of the abdominal aortas stained by hematoxylin and eosin, von Kossa, and ARS. Scale bar: 50 μm. (B) Percentage of calcified area was calculated as the ratio of von Kossa-positive area versus total tissue area. **P<0.01 vs. sham. (C) Representative immunohistochemistry photomicrographs showing Sema4D and Plexin-B1 localization. (D) Sema4D, Plexin-B1, and β-actin levels examined by western blotting. (E) ELISA measurements revealing Sema4D serum levels. **P<0.01 vs. sham. (F) Quantitative real-time PCR results revealing Sema4D and Plexin-B1 mRNA levels. **<0.01 vs. sham.

Figure 2. Sema4D and Plexin-B1 expression during VSMC calcification. Confluent A7r5 and primary VSMCs were exposed to 1.4, 2.6, and 3.5 mM Pi for 7 days with medium change every 2 or 3 days. (A) Absorbance measurements showing the degree of mineralization in calcium deposits within VSMCs stained by ARS. **P<0.01 vs. Cont. (B) Calcium content was measured by colorimetric calcium assay. **P<0.01 vs. Cont. (C) Alkaline phosphatase activity was measured and normalized to protein content for quantitative analysis. **P<0.01 vs. Cont. (D) ELISA results showing Sema4D levels in cell culture medium. *P<0.05, **P<0.01 vs. Cont. (E) Sema4D, Plexin-B1, and β-actin levels examined by western blotting. (D) Quantitative real-time PCR revealing Sema4D and Plexin-B1 mRNA levels. *P<0.05, **P<0.01 vs. Cont.

Figure 3. Effect of Sema4D and Plexin-B1 silencing in phosphate-induced osteogenic differentiation of VSMCs. A7r5 cells were transfected with Sema4D siRNA, Plexin-B1 siRNA or negative control siRNA for 24 h, and then cultured in calcification medium (2.6 mM Pi). After 5 days, VSMC calcification was determined by ARS staining (A), calcium content assay (B), and ALP activity assay (C). **P<0.01 vs. Cont; $^{\#}$P<0.05, $^{\#\#}$P<0.01 vs. siCont. (D) Runx2, calponin, phospho-SMAD1/5, SMAD1/5, and α-tubulin levels examined by western blotting. (E) Immunocytochemistry photomicrographs showing the expression of Runx2 (red) and calponin (green). DAPI staining (blue) denotes nuclear DNA. (F) Quantitative real-time PCR results revealing Runx2 and calponin mRNA levels. *P<0.05, **P<0.01 vs. Cont; $^{\#}$P<0.05, $^{\#\#}$P<0.01 vs. siCont.

Figure 4. Effect of Sema4D and Plexin-B1 knockdown on apoptosis and matrix vesicle release in calcified VSMCs. A7r5 cells were transfected with Sema4D siRNA, Plexin-B1 siRNA or negative control siRNA for 24 h, and then cultured in calcification medium (2.6 mM Pi) for 5 days. (A) Flow cytometry results identifying propidium iodide-positive cells undergoing apoptosis. (B) Representative photographs showing TUNEL-positive apoptotic nuclei (green). DAPI staining (blue) denotes nuclear DNA. Scale bar: 50 μm. (C) Changes in Gas6, Axl, total-/phospho-PI3K, total-/phospho-AKT, Bcl2, and total/cleaved caspase-3 levels as determined by western blotting. (D and E) Matrix vesicles were isolated by collagenase digestion, after which ALP activity was measured and normalized to vesicle total protein content. *P<0.05, **P<0.01 vs. Cont; $^{\#}$P<0.05, $^{\#\#}$P<0.01 vs. siCont.

REFERENCES

1. Singh, A., Tandon, S. and Tandon, C. (2021) An update on vascular calcification and potential therapeutics. Mol. Biol. Rep. 48, 887-896.

2. Leopold, J. A. (2015) Vascular calcification: Mechanisms of vascular smooth muscle cell calcification. Trends Cardiovasc. Med. 25, 267-274.

3. McCarty, M. F. and DiNicolantonio, J. J. (2014) The molecular biology and pathophysiology of vascular calcification. Postgrad. Med. 126, 54-64.

4. Montanaro, M., Scimeca, M., Anemona, L., Servadei, F., Giacobbi, E., Bonfiglio, R., Bonanno, E., Urbano, N., Ippoliti, A., Santeusanio, G., Schillaci, O. and Mauriello, A. (2021) The Paradox Effect of Calcification in Carotid Atherosclerosis: Microcalcification is Correlated with Plaque Instability. Int. J. Mol. Sci. 22, 10.3390/ijms22010395.

5. Masuda, K., Furuyama, T., Takahara, M., Fujioka, S., Kurinami, H. and Inagaki, S. (2004) Sema4D stimulates axonal outgrowth of embryonic DRG sensory neurones. Genes Cells. 9, 821-829.

6. Wang, X., Kumanogoh, A., Watanabe, C., Shi, W., Yoshida, K. and Kikutani, H. (2001) Functional soluble CD100/Sema4D released from activated lymphocytes: possible role in normal and pathologic immune responses. Blood. 97, 3498-3504.

7. Zhang, Y., Liu, B., Ma, Y. and Jin, B. (2013) Sema 4D/CD100-plexin B is a multifunctional counter-receptor. Cell. Mol. Immunol. 10, 97-98.

8. Hu, S. and Zhu, L. (2018) Semaphorins and Their Receptors: From Axonal Guidance to Atherosclerosis. Front. Physiol. 9, 1236.

9. Conrotto, P., Valdembri, D., Corso, S., Serini, G., Tamagnone, L., Comoglio, P. M.,

Bussolino, F. and Giordano, S. (2005) Sema4D induces angiogenesis through Met recruitment by Plexin B1. Blood. 105, 4321-4329.

10. Luque, M. C., Gutierrez, P. S., Debbas, V., Kalil, J. and Stolf, B. S. (2015) CD100 and plexins B2 and B1 mediate monocyte-endothelial cell adhesion and might take part in atherogenesis. Mol. Immunol. 67, 559-567.
11. Wannemacher, K. M., Zhu, L., Jiang, H., Fong, K. P., Stalker, T. J., Lee, D., Tran, A. N., Neeves, K. B., Maloney, S., Kumanogoh, A., Kikutani, H., Hammer, D. A., Diamond, S. L. and Brass, L. F. (2010) Diminished contact-dependent reinforcement of Syk activation underlies impaired thrombus growth in mice lacking Semaphorin 4D. Blood. 116, 5707-5715.
12. Zhu, L., Stalker, T. J., Fong, K. P., Jiang, H., Tran, A., Crichton, I., Lee, E. K., Neeves, K. B., Maloney, S. F., Kikutani, H., Kumanogoh, A., Pure, E., Diamond, S. L. and Brass, L. F. (2009) Disruption of SEMA4D ameliorates platelet hypersensitivity in dyslipidemia and confers protection against the development of atherosclerosis. Arterioscler. Thromb. Vasc. Biol. 29, 1039-1045.
13. Shobeiri, N., Adams, M. A. and Holden, R. M. (2010) Vascular calcification in animal models of CKD: A review. Am. J. Nephrol. 31, 471-481.
14. Jono, S., McKee, M. D., Murry, C. E., Shioi, A., Nishizawa, Y., Mori, K., Morii, H. and Giachelli, C. M. (2000) Phosphate regulation of vascular smooth muscle cell calcification. Circ. Res. 87, E10-7.
15. Park, H. J., Kim, Y., Kim, M. K., Hwang, J. J., Kim, H. J., Bae, S. K. and Bae, M. K. (2020) Inhibition of Gastrin-Releasing Peptide Attenuates Phosphate-Induced Vascular Calcification. Cells. 9, 10.3390/cells9030737.
16. Miyazono, K. (1999) Signal transduction by bone morphogenetic protein receptors:

functional roles of Smad proteins. Bone. 25, 91-93.

17. Proudfoot, D., Skepper, J. N., Hegyi, L., Bennett, M. R., Shanahan, C. M. and Weissberg, P. L. (2000) Apoptosis regulates human vascular calcification in vitro: evidence for initiation of vascular calcification by apoptotic bodies. Circ. Res. 87, 1055-1062.
18. Son, B. K., Kozaki, K., Iijima, K., Eto, M., Nakano, T., Akishita, M. and Ouchi, Y. (2007) Gas6/Axl-PI3K/Akt pathway plays a central role in the effect of statins on inorganic phosphate-induced calcification of vascular smooth muscle cells. Eur. J. Pharmacol. 556, 1-8.
19. Lee, W. P., Wen, Y., Varnum, B. and Hung, M. C. (2002) Akt is required for Axl-Gas6 signaling to protect cells from E1A-mediated apoptosis. Oncogene. 21, 329-336.
20. Stehbens, W. E. (2000) The significance of programmed cell death or apoptosis and matrix vesicles in atherogenesis. Cell. Mol. Biol. (Noisy-le-grand). 46, 99-110.
21. Byon, C. H. and Chen, Y. (2015) Molecular Mechanisms of Vascular Calcification in Chronic Kidney Disease: The Link between Bone and the Vasculature. Curr. Osteoporos Rep. 13, 206-215.
22. Osako, M. K., Nakagami, H., Koibuchi, N., Shimizu, H., Nakagami, F., Koriyama, H., Shimamura, M., Miyake, T., Rakugi, H. and Morishita, R. (2010) Estrogen inhibits vascular calcification via vascular RANKL system: common mechanism of osteoporosis and vascular calcification. Circ. Res. 107, 466-475.
23. Negishi-Koga, T., Shinohara, M., Komatsu, N., Bito, H., Kodama, T., Friedel, R. H. and Takayanagi, H. (2011) Suppression of bone formation by osteoclastic expression of Semaphorin 4D. Nat. Med. 17, 1473-1480.

24. Zhang, Y., Feng, E., Xu, Y., Wang, W., Zhang, T., Xiao, L., Chen, R., Lin, Y., Chen, D., Lin, L., Chen, K. and Lin, Y. (2015) Serum Sema4D levels are associated with lumbar spine bone mineral density and bone turnover markers in patients with postmenopausal osteoporosis. Int. J. Clin. Exp. Med. 8, 16352-16357.

25. Vassalle, C. and Mazzone, A. (2016) Bone loss and vascular calcification: A bi-directional interplay? Vascul Pharmacol. 86, 77-86.

26. Evenepoel, P., Opdebeeck, B., David, K. and D'Haese, P. C. (2019) Bone-Vascular Axis in Chronic Kidney Disease. Adv. Chronic Kidney Dis. 26, 472-483.

27. Chapoval, S. P., Vadasz, Z., Chapoval, A. I. and Toubi, E. (2017) Semaphorins 4A and 4D in chronic inflammatory diseases. Inflamm. Res. 66, 111-117.

28. Wu, J. H., Li, Y. N., Chen, A. Q., Hong, C. D., Zhang, C. L., Wang, H. L., Zhou, Y. F., Li, P. C., Wang, Y., Mao, L., Xia, Y. P., He, Q. W., Jin, H. J., Yue, Z. Y. and Hu, B. (2020) Inhibition of Sema4D/PlexinB1 signaling alleviates vascular dysfunction in diabetic retinopathy. EMBO Mol. Med. 12, e10154.

29. Huang, J., Wu, S., Cao, S., Zhu, X. and Zhang, S. (2020) Neutrophil-Derived Semaphorin 4D Induces Inflammatory Cytokine Production of Endothelial Cells via Different Plexin Receptors in Kawasaki Disease. Biomed. Res. Int. 2020, 6663291.

30. Davenport, C., Harper, E., Forde, H., Rochfort, K. D., Murphy, R. P., Smith, D. and Cummins, P. M. (2016) RANKL promotes osteoblastic activity in vascular smooth muscle cells by upregulating endothelial BMP-2 release. Int. J. Biochem. Cell Biol. 77, 171-180.

31. Bouabdallah, J., Zibara, K., Issa, H., Lenglet, G., Kchour, G., Caus, T., Six, I., Choukroun, G., Kamel, S. and Bennis, Y. (2019) Endothelial cells exposed to phosphate and indoxyl sulphate promote vascular calcification through interleukin-8

secretion. Nephrol. Dial. Transplant. 34, 1125-1134.

32. Meng, F., Zhao, Y., Wang, B., Li, B., Sheng, Y., Liu, M., Li, H. and Xiu, R. (2018) Endothelial Cells Promote Calcification in Aortic Smooth Muscle Cells from Spontaneously Hypertensive Rats. Cell. Physiol. Biochem. 49, 2371-2381.

33. Liu, E. S., Chen, N. C., Jao, T. M. and Chen, C. L. (2021) Dextromethorphan Reduces Oxidative Stress and Inhibits Uremic Artery Calcification. Int. J. Mol. Sci. 22, 10.3390/ijms222212277.

34. Zhao, M. M., Xu, M. J., Cai, Y., Zhao, G., Guan, Y., Kong, W., Tang, C. and Wang, X. (2011) Mitochondrial reactive oxygen species promote p65 nuclear translocation mediating high-phosphate-induced vascular calcification in vitro and in vivo. Kidney Int. 79, 1071-1079.

35. Toth, A., Balogh, E. and Jeney, V. (2020) Regulation of Vascular Calcification by Reactive Oxygen Species. Antioxidants (Basel). 9, 10.3390/antiox9100963.

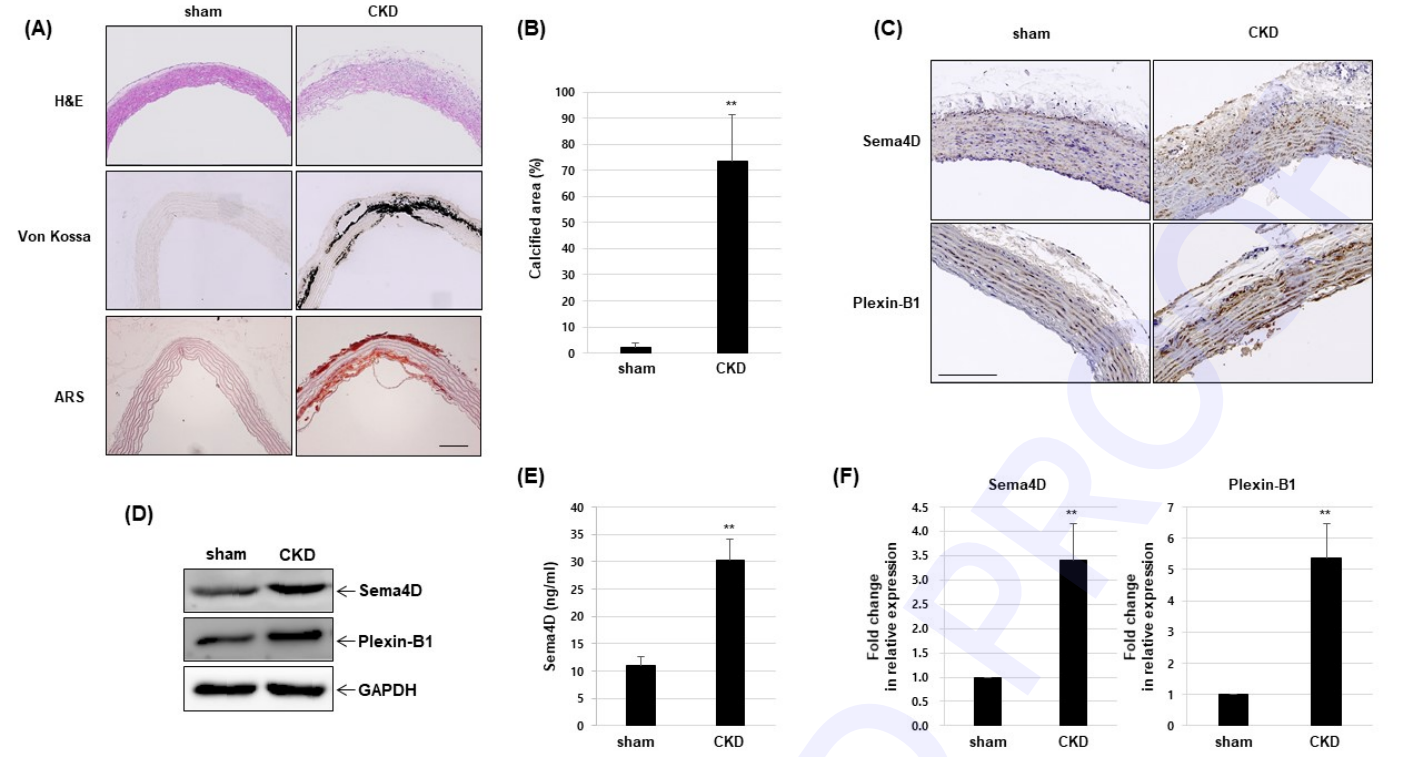

Fig. 1.

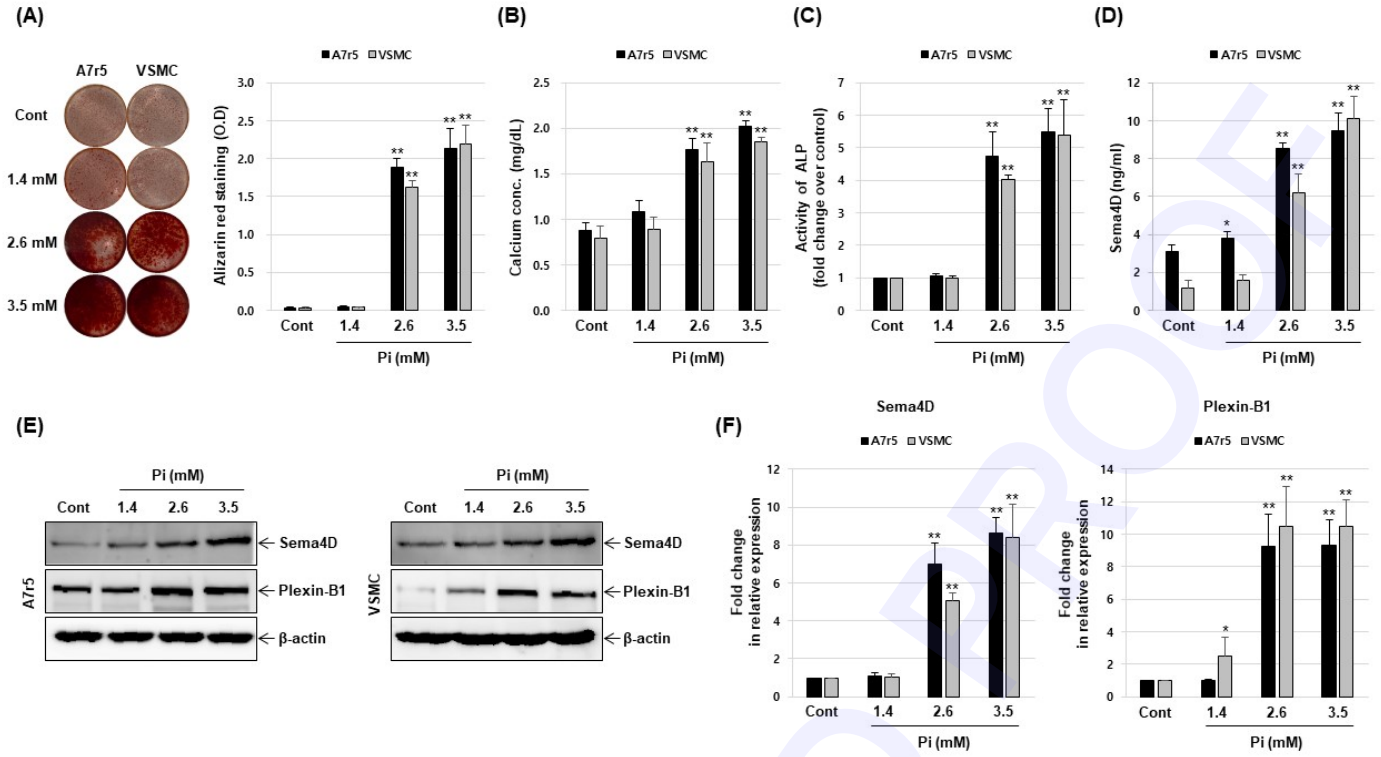

Fig. 2.

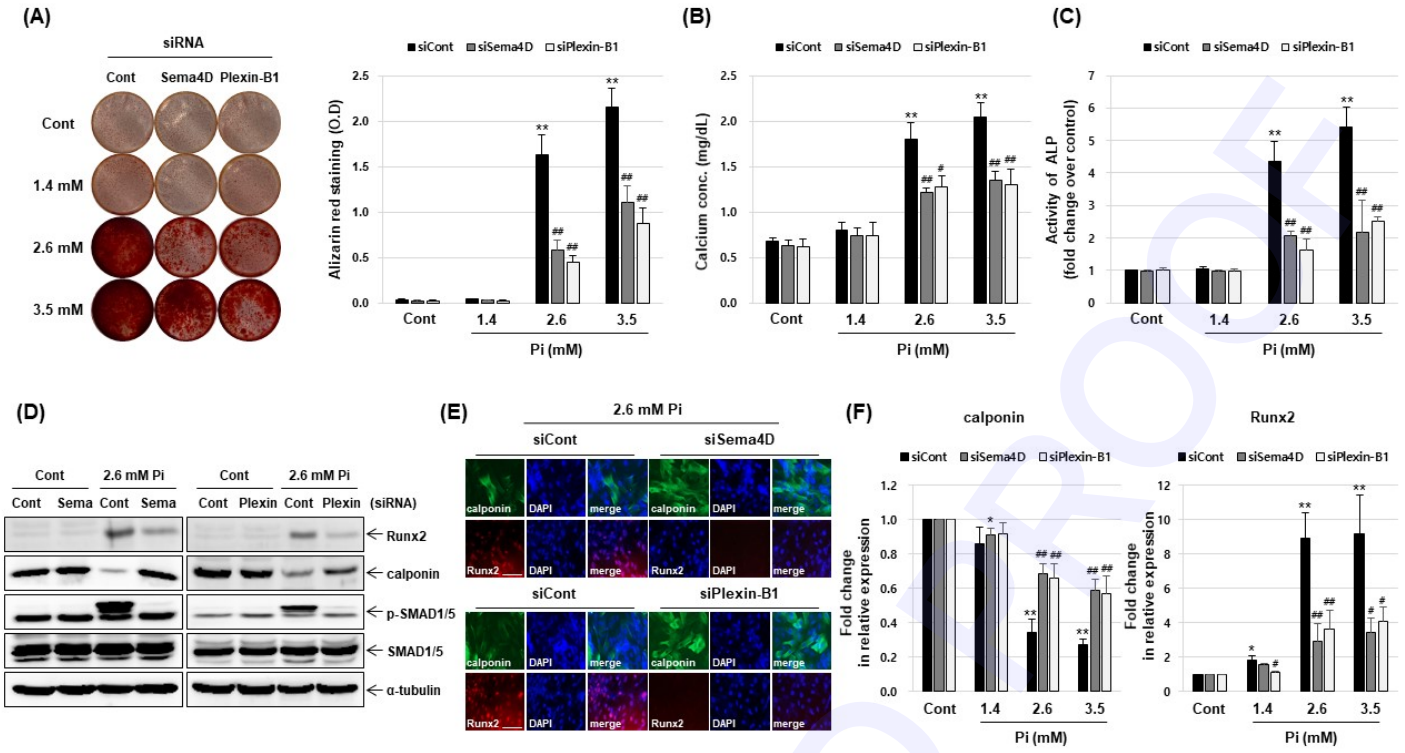

Fig. 3.

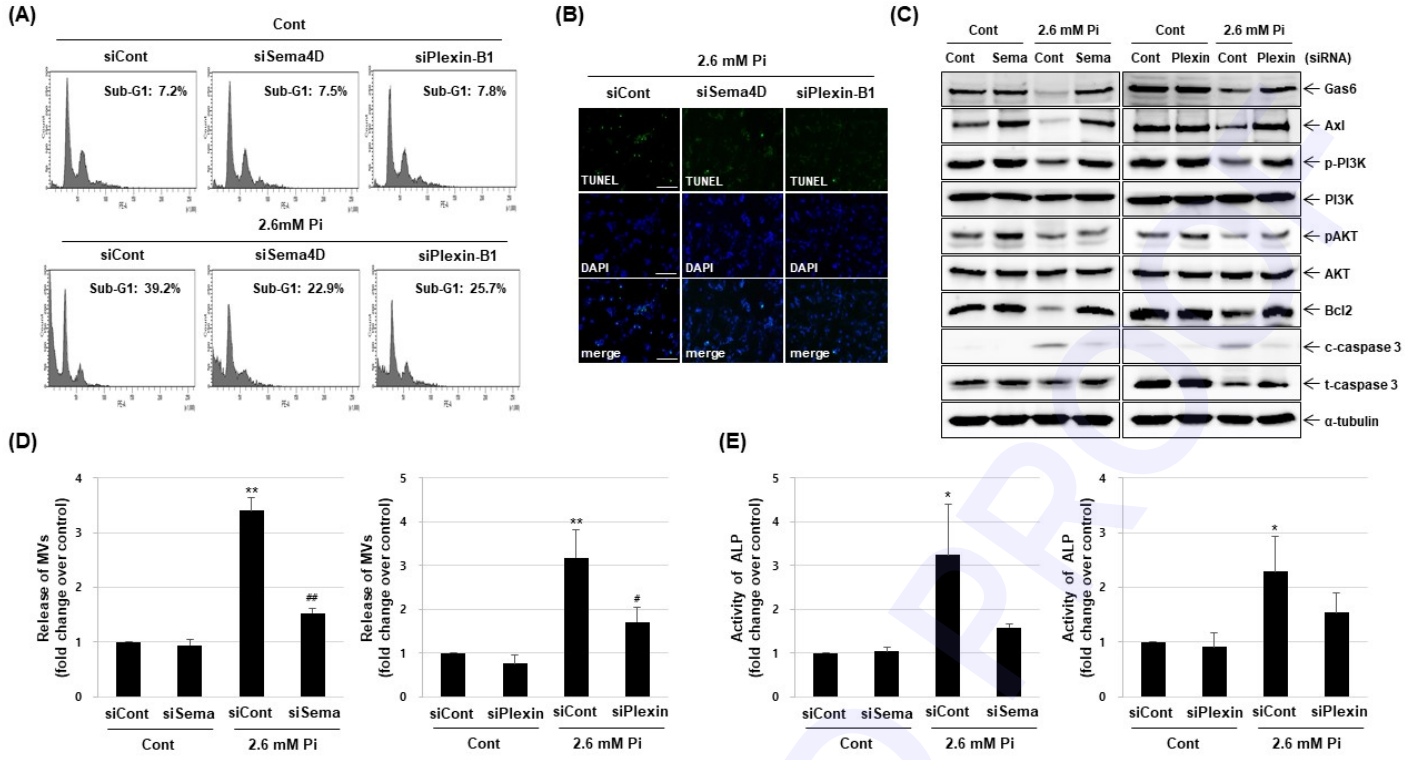

Fig. 4.

Title: Inhibition of the Semaphorin 4D-Plexin-B1 axis prevents calcification in vascular smooth muscle cells

Author's name: Hyun-Joo Park[1,2,3], Yeon Kim[1,2,3], Mi-Kyoung Kim[1,2], Hyung Joon Kim[1,2,3], Soo-Kyung Bae[2,3,4], and Moon-Kyoung Bae[1,2,3*]

Affiliation: [1]Department of Oral Physiology, [2]Periodontal Disease Signaling Network Research Center (MRC), [3]Dental and Life Science Institute, [4]Department of Dental Pharmacology, School of Dentistry, Pusan National University, Yangsan 50612, South Korea

Supplementary Information

The following file contains supplementary material for the paper "Inhibition of the Semaphorin 4D-Plexin-B1 axis prevents calcification in vascular smooth muscle cells".

This file is composed of:

- Supplementary figures and relative supplementary figure legends (3 figures)
- Supplementary tables (2 tables)
- Materials and methods
- References

Supplementary Figures

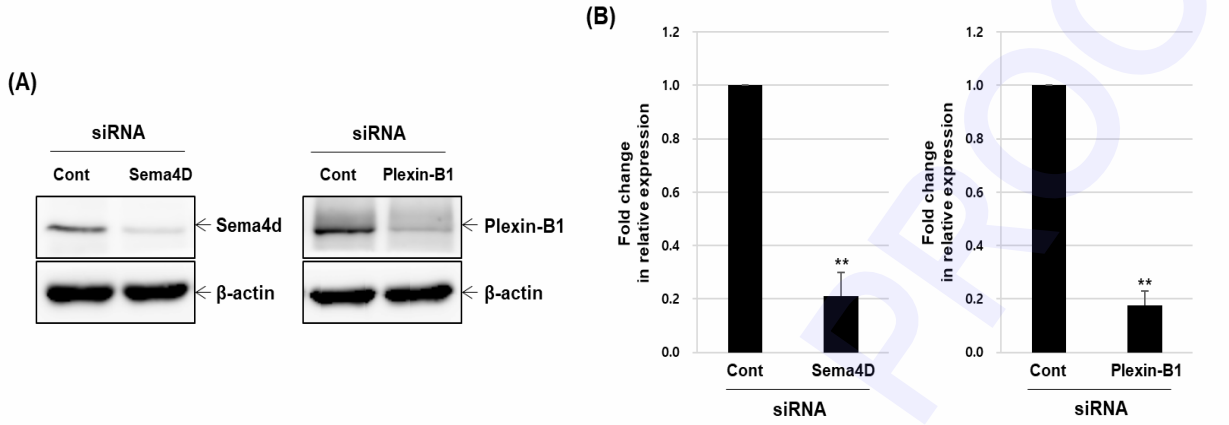

Supplementary Fig 1. Effect of Sema4D and Plexin-B1 knockdown in A7r5 cells. Cells were transfected with Sema4D siRNA, Plexin-B1 siRNA or negative control siRNA for 48 h. (**A**) Sema4D and Plexin-B1 protein level was examined by western blotting using their corresponding antibodies. (B) Using real-time RT-PCR, the expression level of Sema4D and Plexin-B1 was also quantified. **P<0.01 vs. control siRNA. Data shown are the mean ± SD, obtained for at least three independent experiments.

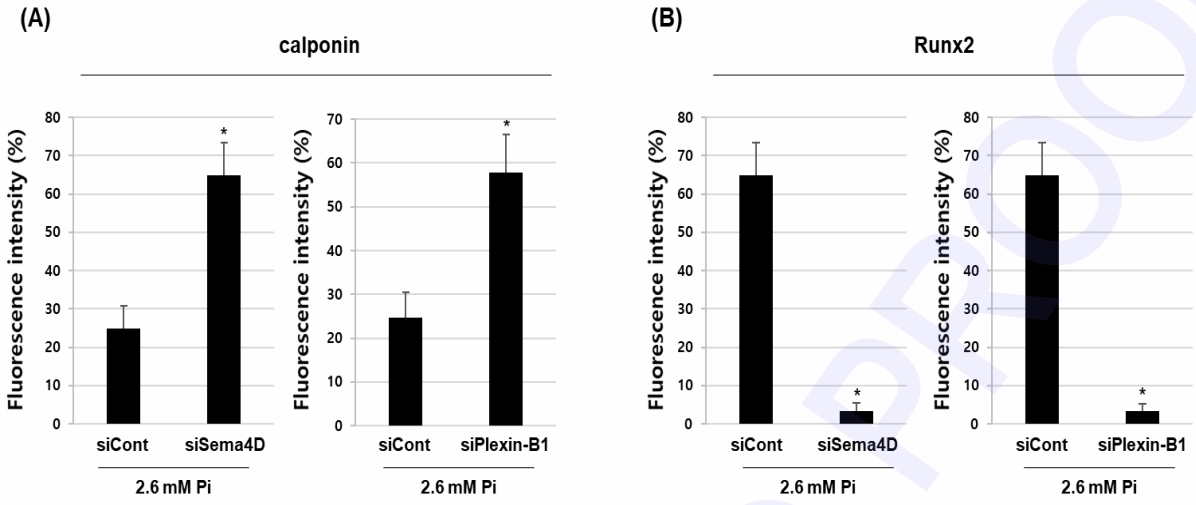

Supplementary Fig 2. The quantitative analysis of immunofluorescence intensity. A7r5 cells were transfected with Sema4D siRNA, Plexin-B1 siRNA or negative control siRNA for 24 h, and then cultured in calcification medium (2.6 mM Pi) for 5 days. Calponin (green) and Runx2 (red) positive cells were expressed as a percentage of the total number of DAPI-stained nuclei (blue). The percentage of calponin and Runx2 positive cells was showed as mean ± SD (n = 3, each). *P<0.05 vs. control siRNA.

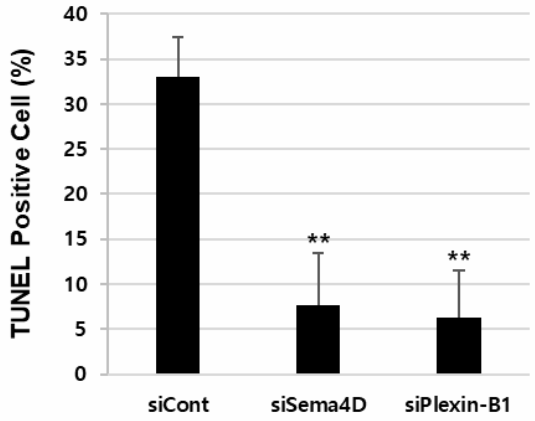

Supplementary Fig 3. The quantitative analysis of percentage of TUNEL positive cells. A7r5 cells were transfected with Sema4D siRNA, Plexin-B1 siRNA or negative control siRNA for 24 h, and then cultured in calcification medium (2.6 mM Pi) for 5 days. TUNEL positive cells (green) were expressed as a percentage of the total number of DAPI-stained nuclei (blue). The percentage of TUNEL positive cells (apoptotic cells) was showed as mean ± SD (n = 3, each). **P<0.01 vs. control siRNA.

Supplementary Tables

Study groups	n	Body weight (g)	BUN (mg/dl)	Creatinine (mg/dl)	Phosphate (mmole/l)	Calcium (mg/dl)
sham	4	323.47±4.07	14.51±2.68	0.29±0.03	2.55±0.42	9.21±0.13
CKD	6	249.89±5.46	162.09±5.24**	2.73±0.42**	4.68±1.08*	10.51±1.79

Supplementary Table 1. Physical and biochemical parameters in CKD rats. CKD rats were fed a diet supplemented with 0.75% adenine for 8 weeks. Body weight, and the serum levels of blood urea nitrogen (BUN), creatinine, phosphate, and calcium in each group of mice were measured using colorimetric assay kits. *P<0.05, **P<0.01 vs. sham. Data shown are the mean ± SD, obtained for at least three independent experiments.

Genes	Accession No.	Sequences (5′ → 3′)	Length(bp)
β-actin	NM_031144.3	Forward: AGGGAAATCGTGCGTGAC Reverse: CGCTCATTGCCGATAGTG	146bp
Sema4D	NM_001109149.1	Forward: TGGGAGCACGGAGAGGTAGG Reverse: CTTCCCGGGCACCCACATAC	112bp
Plexin-B1	NM_001108188.2	Forward: GGACAGAGACTGTGGTGGAA Reverse: TCCTACAGAGTCCCTCACGA	80bp
Runx2	NM_001278483.1	Forward: GCCGGGAATGATGAGAACTA Reverse: TGGGGAGGATTTGTGAAGAC	155bp
calponin	D14437.1	Forward: GAACAAGCTGGCCCAGAAAT Reverse: GGCCATCCATGAAGTTGCTC	104bp

Supplementary Table 2. Primer sequences for real-time RT-PCR.

Materials and methods

Induction of CKD rat model

CKD was induced as described previously (1). Twelve-week-old male Wistar rats (Orientbio) were randomly divided into two groups: sham and CKD. Animals from the sham group were fed a normal diet; whereas those from the CKD group were fed a diet supplemented with 0.75% adenine for 8 weeks. All animal experiments were conducted in accordance with the Guide for the Care and Use of Laboratory Animals (NIH publication No. 85-23, revised 1996) and were approved by the Institutional Animal Care and Use Committee at Pusan National University, Korea.

Von Kossa staining

After dewaxing in xylene and rehydrating through a graded alcohol series, slides with tissue slices were soaked in distilled water and incubated in 1% silver nitrate solution (Sigma Aldrich Co.) under an ultra violet lamp for 15 min. They were subsequently soaked in 5% sodium thiosulfate for 5 min and cleaned with distilled water, after which the sections were incubated with nuclear fast red for 5 min at 23–25°C and dehydrated using a graded alcohol series.

Alizarin red S (ARS) staining

Samples were fixed with 4% paraformaldehyde, stained with 1 mg/ml ARS (Sigma Aldrich Co.)

solution for 30 min at 37°C, rinsed, and photographed. Then, the calcium deposits were destained, dissolved in 10% acetic acid, and the calcification was quantified by measuring the absorbance at 420 nm using a multi-detection microplate reader (Dynex).

Antibodies

Antibodies against Sema4D and Plexin-B1 were supplied by Santa Cruz Biotechnology. Antibodies against phospho-Smad1/5, phospho-/total-Akt, phospho-/total-PI3K, total/cleaved caspase-3, Runx2, and those for Bcl2 were obtained from Cell Signaling. Antibodies against calponin and Gas6 were purchased from Abcam. Antibodies against Smad1/5 and Axl, as well as horseradish peroxidase-conjugated goat anti-mouse and anti-rabbit IgG were procured from Thermo Fisher Scientific.

Immunohistochemistry

Sectioned paraffin-embedded tissues were deparaffinized, and incubated in phosphate-buffered saline (PBS) containing 0.3% H_2O_2. The tissue sections were then blocked with 1% bovine serum albumin, and incubated with anti-primary antibodies. The sections were incubated with the Envision Detection System (DAKO), counterstained with hematoxylin, mounted in Vectamount (Vector Labs), and photographed using an Axio Scan.Z1 Slide Scanner (ZEISS).

Western blot analysis

Harvested cells were lysed in a RIPA buffer (Sigma Aldrich Co.). Proteins (30 μg/lane) were separated by SDS/PAGE and transferred to nitrocellulose membranes (GE Healthcare Life Sciences). Membranes were blocked for 60 min with 5% skim milk in Tris-buffered saline containing 0.1% Tween-20 and probed with the appropriate antibodies. The signal was detected by enhanced chemiluminescence (GE Healthcare Life Sciences).

ELISA

The amount of secreted Sema4D protein was determined by ELISA following the manufacturer's instructions (MyBioSource). Absorbance at 450 nm was measured using an ELISA reader (Dynex), and Sema4D levels were determined by interpolating the values onto a standard curve generated according to the manufacturer's instructions.

Quantitative real-time PCR

Quantitative real-time PCR was performed using SYBR Green (Roche Applied Science). Amplifications included one cycle at 95°C for 10 min, followed by 30 cycles at 95°C for 10 s, 57°C for 5 s, and 72°C for 7 s. The entire amplification process including data analysis took less than 60 min and was monitored using the Light Cycler software (version 4.0). Oligonucleotide primer sequences are listed in Supplementary Table 2.

Cell isolation and culture

VSMCs were isolated from thoracic aortas of male Sprague–Dawley rats (3-week-old; Samtaco) (2). The smooth muscle A7r5 cell line was purchased from the American Type Culture Collection (CRL-1444^{TM}). Primary VSMCs and A7r5 cells were grown in Dulbecco's modified Eagle medium (DMEM; Gibco) with 10% fetal bovine serum (Gibco) and 1% antibiotics (Gibco) at 37°C in a humidified 95% air and 5% CO_2 environment.

Induction and quantification of calcification

A solution of Pi (Na_2HPO_4 and NaH_2PO_4, pH 7.4) was added to serum-supplemented DMEM at a final concentration of 1.4, 2.6, and 3.5 mM. After the indicated incubation period, cellular calcium content and ALP activity were determined using a calcium colorimetric assay kit (BioVision) and an ALP assay kit (TaKaRa Bio), respectively.

Gene knockdown by siRNA

The siRNA duplexes for rat Sema4d, Plexin-B1, and a negative control siRNA were bought from GenePharma. VSMCs were transfected using the Amaxa Nucleofector technology (Lonza) according to the manufacturer’s instructions.

Immunocytochemistry

Cells grown on coverslips were fixed in 4% paraformaldehyde for 10 min, washed with 0.5% Triton X-100 in PBS for 5 min, and then incubated with appropriate primary antibodies, followed

by incubation with secondary antibodies conjugated with Alexa® 488 and Alexa® 594. Coverslips were mounted in Vectastain containing 4′,6-diamidino-2-phenylindole (DAPI; Vector Laboratories). Images were recorded using a fluorescence microscope (Nikon).

Flow cytometry analysis

VSMCs were incubated in a calcification medium for 7 days, washed twice in 1× PBS, and fixed in chilled 70% ethanol. The cells were stained with 5 μg/ml propidium iodide (Sigma Aldrich Co.) at 23–25°C for 10 min, and analyzed using a FACSCalibur flow cytometer (BD Bioscience). The cell cycle profile was determined with the Modfit LT software.

TUNEL assay

Apoptotic cells were detected using the DeadEnd^{TM} Fluorometric TUNEL System (Promega) in accordance with the manufacturer's instructions. Cells were incubated in calcification medium for 7 days, fixed in 4% paraformaldehyde for 25 min at 4°C, and permeabilized with 0.2% Triton X-100 for 5 min at room temperature. Free 3′-ends of the fragmented DNA were labeled in the TUNEL reaction mixture for 60 min at 37°C in a humidified chamber and visualized under a fluorescence microscope (Nikon).

Matrix vesicle isolation

Matrix vesicles were harvested following a modified matrix vesicle isolation protocol (3).

Confluent VSMCs were washed twice with PBS and transferred to control or calcification medium for 7 days. Then, the medium was decanted after digestion with collagenase and centrifuged at 10,000 × *g* to remove the cells and apoptotic bodies. Matrix vesicles were harvested from the supernatant by centrifugation at 100,000 × *g* for 30 min at 4°C in an ultracentrifuge (Beckman Coulter), resuspended in 1% Triton X-100, and the activity of the protein and ALP were determined. Increased protein levels indicated a larger number of matrix vesicles.

Statistical analyses

Data represent the mean standard deviation calculated for at least three independent repetitions of the experiments. The data was subjected to analysis by one-way ANOVA with Tukey's honestly significant difference (HSD) post hoc test and student's t test.

References

1. Shobeiri, N., Adams, M. A. and Holden, R. M. (2010) Vascular calcification in animal models of CKD: A review. Am. J. Nephrol. 31, 471-481.

2. Park, H. J., Kim, M. K., Kim, Y., Kim, H. J., Bae, S. K. and Bae, M. K. (2021) Neuromedin B modulates phosphate-induced vascular calcification. BMB Rep. 54, 569-574.

3. Reynolds, J. L., Joannides, A. J., Skepper, J. N., McNair, R., Schurgers, L. J., Proudfoot, D., Jahnen-Dechent, W., Weissberg, P. L. and Shanahan, C. M. (2004) Human vascular smooth muscle cells undergo vesicle-mediated calcification in response to changes in extracellular calcium and phosphate concentrations: a potential mechanism for accelerated vascular calcification in ESRD. J. Am. Soc. Nephrol. 15, 2857-2867.